European Commission

JRC TECHNICAL REPORTS

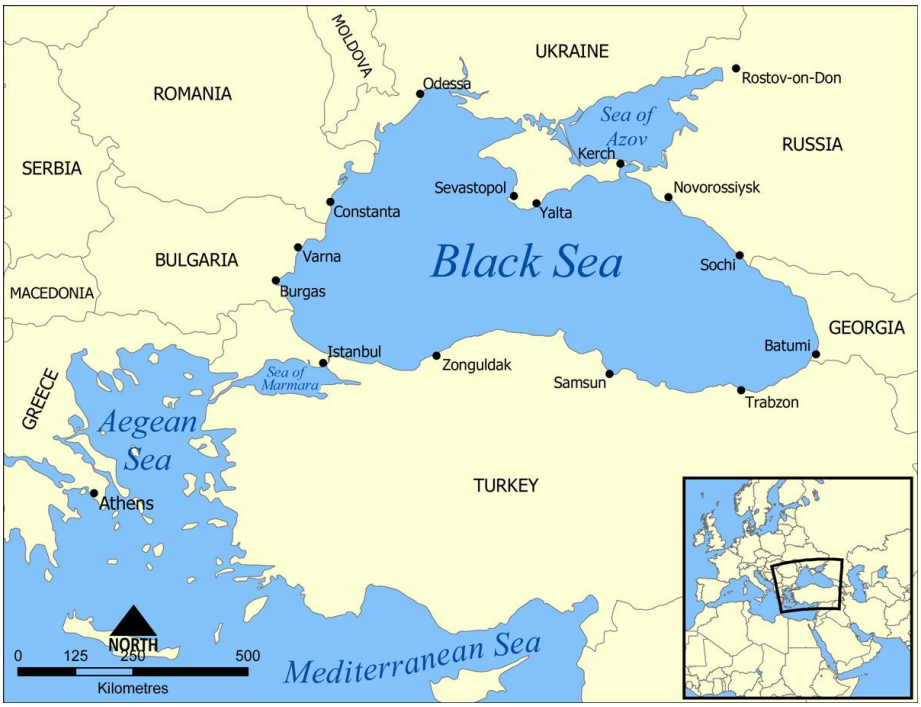


# Development of the Black Sea specific Ecosystem model (BSSM)

Temel Oguz
Adolf Stips
Diego Macias Moy
Elisa Garcia-Gorriz
Clare Coughlan

2014

Report EUR 27003 EN

Joint Research Centre

European Commission
Joint Research Centre
Institute for Environment and Sustainability

Contact information
Adolf Stips
Address: Joint Research Centre, Via Enrico Fermi 2749, TP 272, 21027 Ispra (VA), Italy
E-mail: adolf.stips@jrc.ec.europa.eu
Tel.: +39 0332 78 9876

JRC Science Hub
https://ec.europa.eu/jrc



JRC 93252

EUR 27003 EN

ISBN 978-92-79-44670-2 (PDF)

ISSN 1831-9424 (online)

doi:10.2788/82470

Luxembourg: Publications Office of the European Union, 2014



Abstract

In the context of implementing and revising the European Marine Strategy Framework Directive (MSFD), modelling work has been initiated to assess the status and trends of the Black Sea marine ecosystem. This initiative involves development of a coupled physical-ecosystem modelling system by implementing online coupling between GETM/GOTM and Black Sea Specific ecosystem Model (BSSM), developed by Prof. Temel Oguz. A series of experiments was carried out to fine-tune model response to the forcing mechanisms in the Black Sea and a nitrate-based biogeochemical model has been implemented. Further work will include horizontal variability to the coupled system.

## 1. Introduction/background

In the context of implementing and revising the European Marine Strategy Framework Directive (MSFD), modelling work has been initiated to assess the status and trends of the Black Sea marine ecosystem. This initiative involves development of a coupled physical-ecosystem modelling system by implementing online coupling between GETM/GOTM and Black Sea Specific ecosystem Model (BSSM), developed by Prof. Temel Oguz.

## 2. Progress of the project (activities undertaken, methods, materials, developments) and the results

### *2.1 Hydrodynamic model and test runs*

A series of experiments has been carried out to systematically study the model response to the forcing mechanisms in the Black Sea. First, a satisfactory vertical distribution of sigma layers was obtained (section 2a). Then the model was run with no external forcing while testing the effects of topographic smoothing to reduce the pressure gradient error introduced by the sigma coordinates (sections 2b and 2c). At the same time, values for the horizontal diffusion coefficient were tested. The model was run with only rivers forcing (Danube, Dniepr and Dniestr) and straits (Bosphorus and Kerch) to examine their contribution to the development of buoyancy-induced currents around the basin (section 2d). This run was then extended to include horizontally uniform heat and salt flux forcing (section 2e).

#### *Adjustment of sigma levels depending on the vertical stratification within the upper 200 m layer*

The basic idea is to find the best possible vertical distribution of sigma levels that reduces the cumulative pressure gradient error estimated over the whole domain, at the same time retaining sufficient resolution in the upper layer, at the topographic slope zone and at the bottom boundary layer. In GETM it is possible to zoom the upper and lower layers of the sigma levels. We tried various settings (***Figure 1:*** *sigma layer distribution at [31.8 N, 43.0 E] for different zooming parameters* ***Figure 1***) to match the optimum distribution; ddu = 3, ddl = 1(yellow line) by allowing 9 layers in the top 50 m (***Figure*** 2a), and approximately 100 m resolution near the bottom (***Figure 2***b).

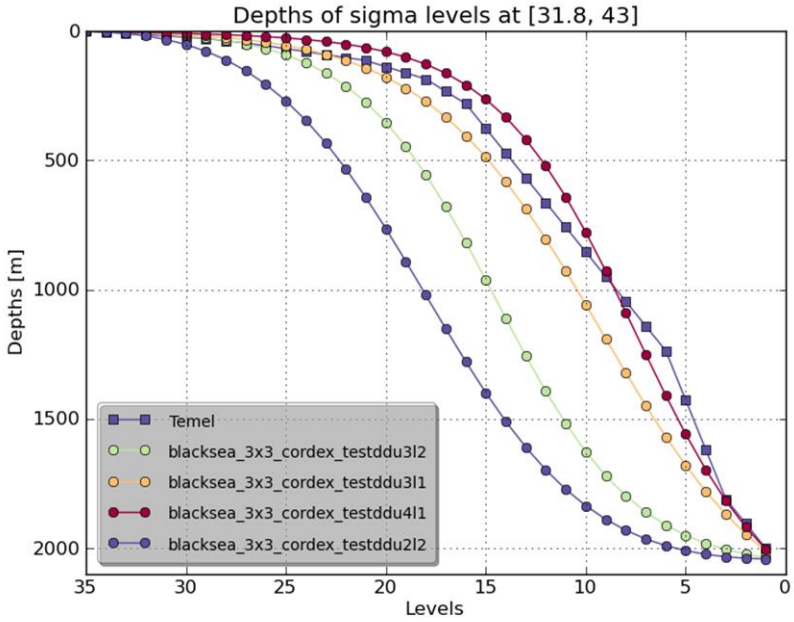


***Figure 1:*** *sigma layer distribution at [31.8 N, 43.0 E] for different zooming parameters. The yellow line gives the optimum distribution.*

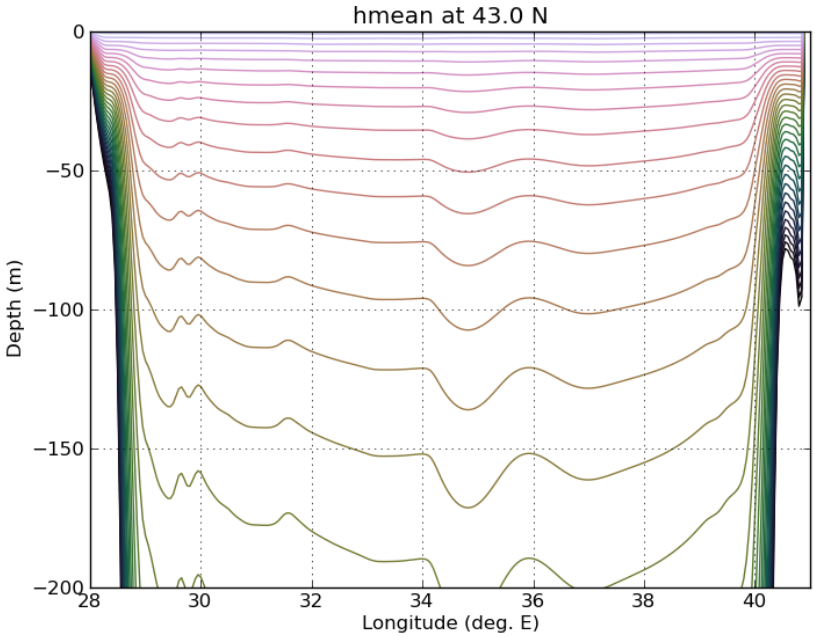


***Figure 2a:*** *sigma layer distribution in the top 200 m across 43 N*

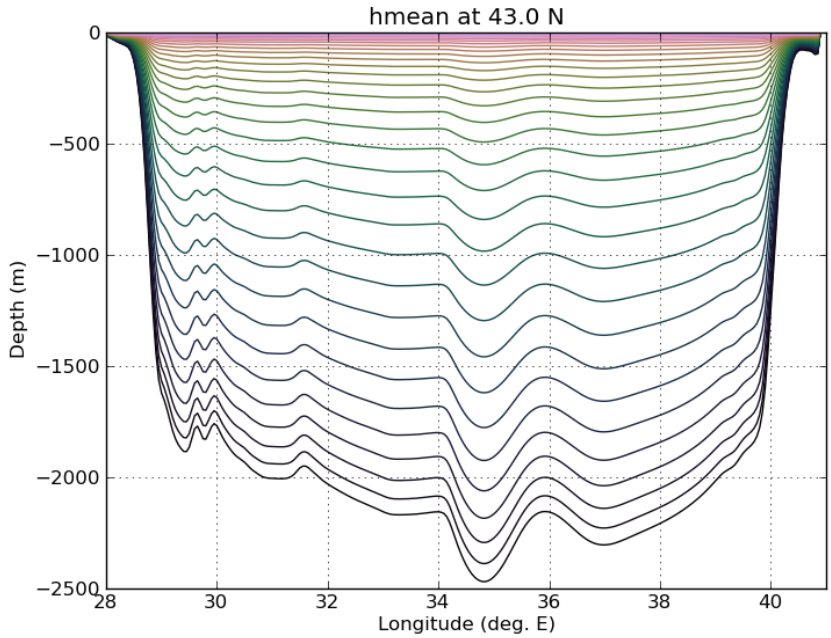


***Figure 2b:*** *full sigma layer distribution across 43 N*

***Adjustment and smoothing of topography for reducing the pressure gradient error introduced by the sigma coordinate***

As a limitation of the sigma coordinate system in ocean circulation models the real topography needs to be smoothed to reduce error introduced by extraordinarily steep topographic slopes. We therefore invested efforts to vary the level of smoothing of the topography and measured the error introduced by the smoothings. The optimum choice found with the parameters (slpmax rmax = 0.5, centered smoothing routine) is shown in Figure 3. This choice reduces the error in the steep topographic slope zone to less than 4 cm/s at 500 m depth.

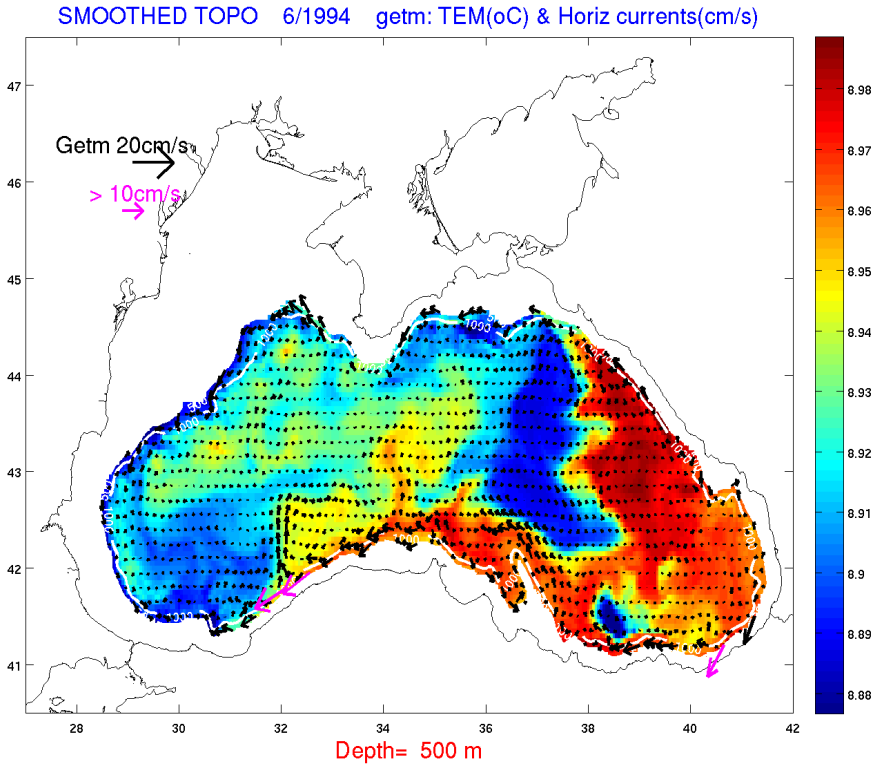


***Figure 3:*** *Modelled currents and temperature at 500 m; no model forcing*

### *Running the model without any forcing*

After deciding on the distribution of sigma coordinates and smoothed topography a series of simulations was performed to select the optimum value of the horizontal diffusion coefficient. The range of horizontal diffusivity tested was [10, 100] and its optimum value chosen was 30 $m^2/s$.

### *Running the model only with the river fluxes to examine their contribution to buoyancy-induced current around the basin.*

A further test on the performance of the model was done by including only the major rivers discharging onto the north western coast of the Black Sea (Danube, Dniepr, Dniestr). The motivation of this simulation was to assess the performance of the model to reproduce buoyancy driven boundary current around the Black Sea. As shown in Figure 4, the model was able to reproduce the Black Sea rim current successfully.

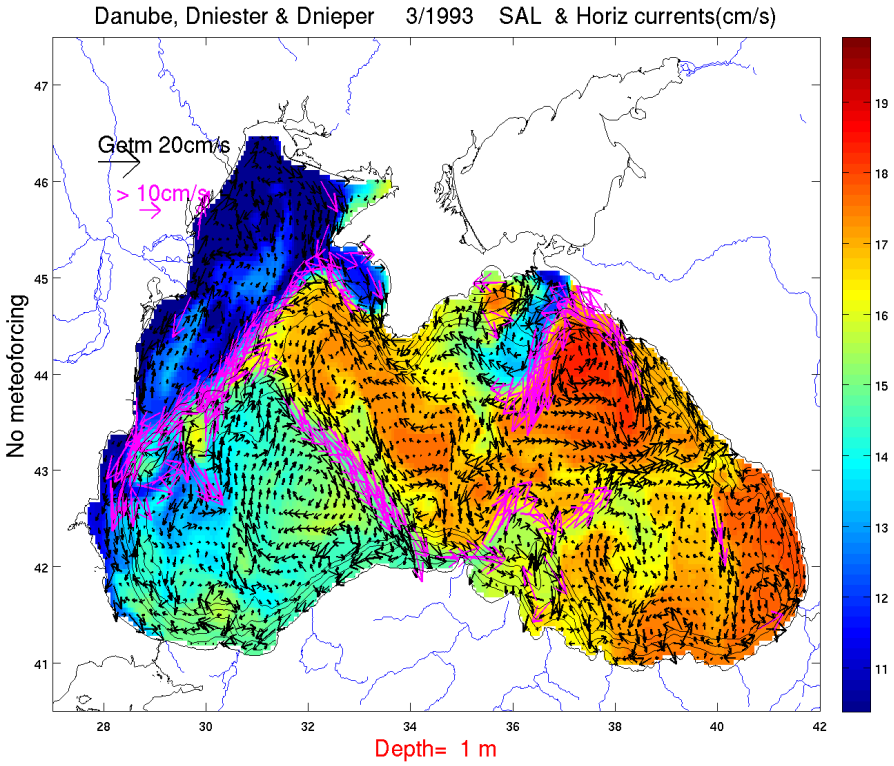


***Figure 4:*** *Modelled salinity and currents at the surface, 3 rivers included.*

***Running the model with single year (but horizontally averaged forcing) and getting a perpetual year solution.***

The previous run is then extended to include horizontally uniform heat flux for the year 1998. The model is run with fresh water fluxes as well as perpetual yearly forcing of heat flux for 10 years. That simulation was intended to test the performance of the model for mixed layer evolution during the year, for example, cold water mass formation during winter and formation of the strong seasonal thermocline in summer. The June pattern of horizontal circulation at the surface as well as the zonal temperature transects across the basin for March and July are shown in Figures 5a, 5b and 5c. The outcome of the simulation demonstrates the capability of the model to produce the observed thermohaline structure.

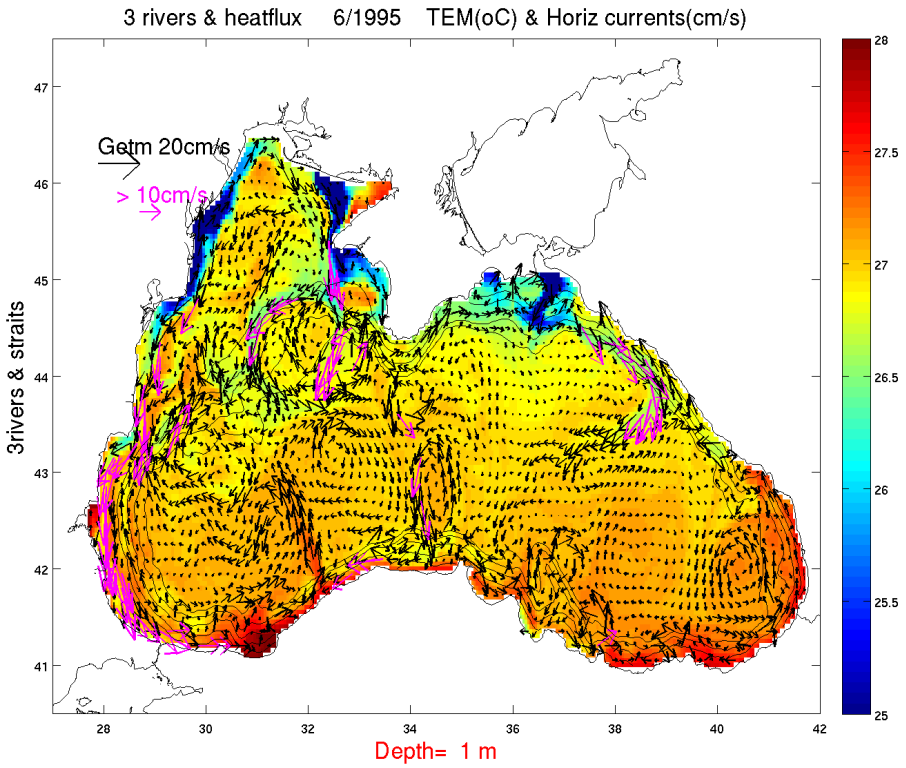


***Figure 5a:*** *modelled temperature and horizontal currents for June 1995; model forcing includes 3 rivers and horizontally averaged heat flux*

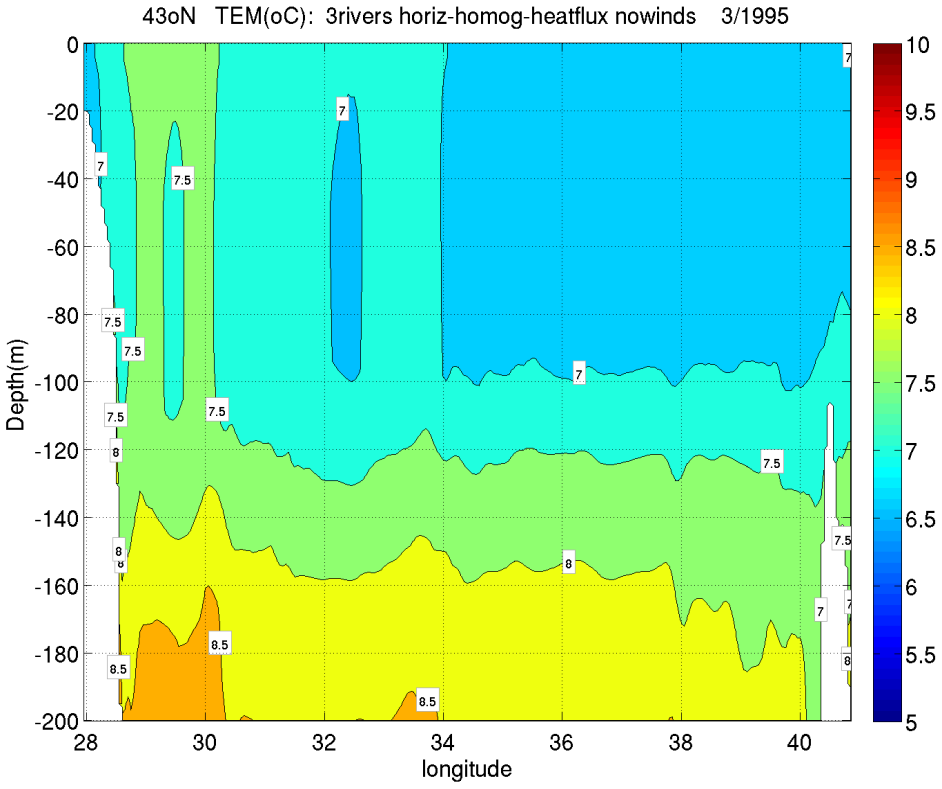


***Figure 6b:*** *zonal temperature structure in March 1995; model forcing includes 3 rivers and horizontally averaged heat flux*

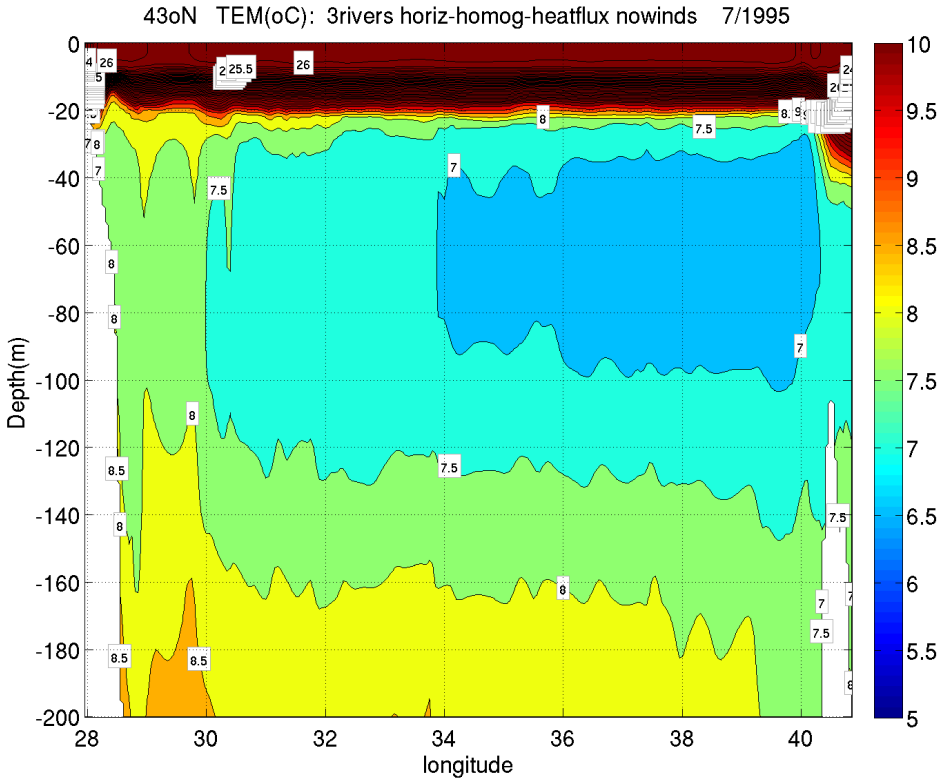


***Figure 7c:*** *zonal temperature structure in July 1995; model forcing includes 3 rivers and horizontally averaged heat flux*

As a further extension of the previous simulation horizontally averaged freshwater flux was included in addition to the other forcings. The motivation was to see if the model would be able to reproduce more realistic coastal to interior basin salinity contrast. Figure 5d shows that with proper thermohaline forcing and prescribed river water fluxes the model can reproduce the main features of the Black Sea circulation, even under such simplified settings.

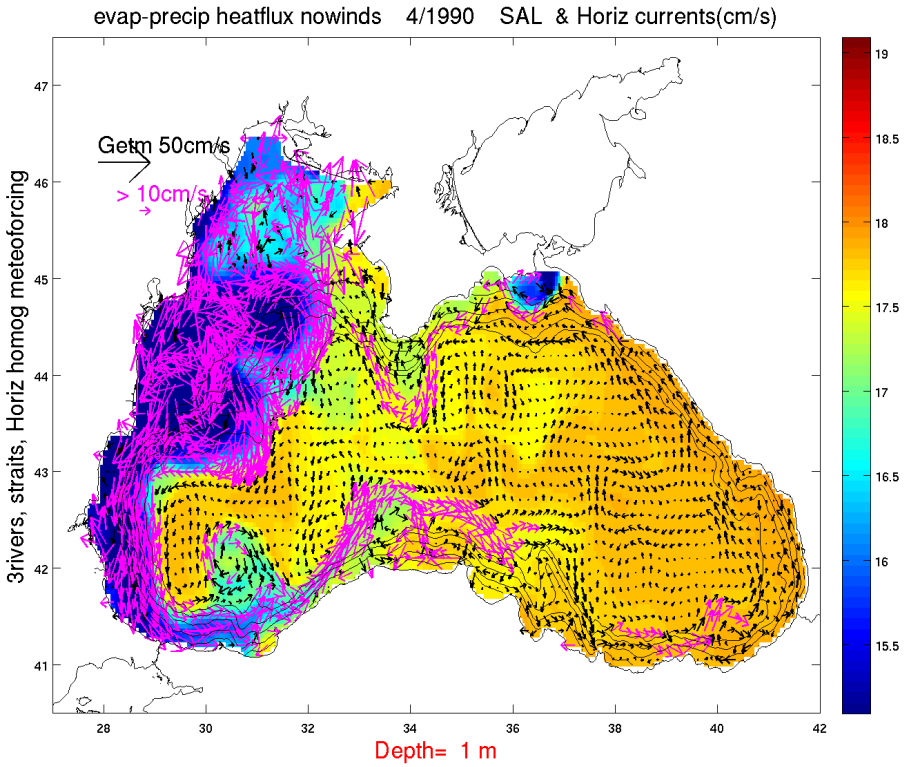


***Figure 8d:*** *modelled salinity and horizontal currents for April 1990; model forcing includes 3 rivers and horizontally averaged heatflux, evaporation and precipitation*

### *2.2 Ecosystem model description*

To describe the lower-trophic level pelagic ecosystem model of the Black Sea, a nitrate-based biogeochemical model has been implemented following the existing literature (e.g., Oguz et al., 2000, 2001, 2006, 2008). This model provides an optimally complex system of food web interactions and biogeochemical cycles comprising oxic-, suboxic- and anoxic waters of the Black Sea. It represents the classical omnivorous food-web with 7 state variables. These include two phytoplankton size groups (small and large), four zooplankton groups including micro- and mesozooplankton, non-edible dinoflagellate species as *Noctiluca,* and the gelatinous zooplankton species *Mnemiopsis.* The nitrogen cycle is modelled by particulate organic material (detritus compartment) and two inorganic nutrients (nitrate and ammonium). Additional state variables are dissolved oxygen and hydrogen sulphide. This system offers an optimal complexity with very complex trophic interactions as shown in Figure 6. The full set of equations describing this ecosystem is provided in Appendix A. Hereinafter this model will be referred to as BSSM ecosystem model.

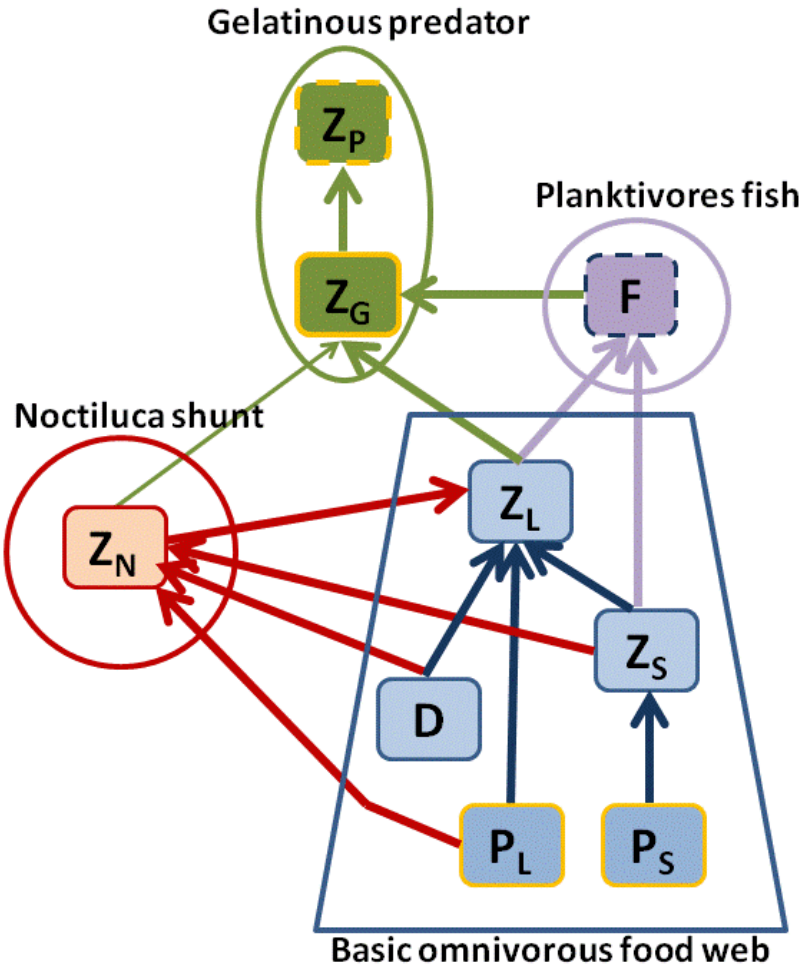


***Figure 9:*** *Schematic representation of the model food web structure that comprises the basic omnivorous food web and its interactions with the planktivores fish (denoted by F) and the gelatinous carnivore predators (denoted by ZP) as well as the Noctiluca shunt (denoted by $Z_N$). The mesozooplankton group supports both the fish and gelatinous predator groups and competes for the same food sources with Noctiluca which shunts a part of food energy from mesozooplankton.*

#### *2.3 Implementation of ecosystem model to FABM*

BSSM ecosystem model has been successfully implemented into the *Framework for Aquatic Biochemical Models* (FABM) coupler. FABM is an interface between biogeochemical models and physical models created to work with the *General Estuarine Transport Model* (GETM) being used at JRC. Model tests are in progress to finalise the choice of parameterisations for consistency with the GETM/GOTM circulation model. The model has been compiled and is running without horizontal variability but retaining the vertical structure (1D structure). More work is still needed to elaborate the programming and coupling aspects of the model.

#### *2.4 Initial outputs from ecosystem model*

Coupling with the *General Ocean Turbulent Model* (GOTM) physical model, the 1D BSSM ecosystem model using atmospheric forcing extracted from the reanalysis datasets at a central location within the BS (43.1°N, 32.6°E), temperature and salinity profiles

extracted from the world ocean atlas (2009), and initial profiles from Stanev et al (2014) is run for 11 years to reach the perpetual equilibrium state for the time period 1990 to 2000. The results of this particular simulation are shown in Figures 7a – 7d. The model was shown to reproduce correct nitrogen cycling and vertical structure in addition to the realistic profiles of hydrogen sulphide and oxygen concentrations (Figure 7a). The annual phytoplankton biomass is dominated by the large phytoplankton group in winter/spring and the small phytoplankton group in summer, as observed (Figure 7b). The model also reproduced correct blooming periods of *Noctiluca* and *Mnemiopsis* (figure 7c). A summary of these vertically structured annual variations is provided in Figure 7d in terms of depth-integrated quantities.

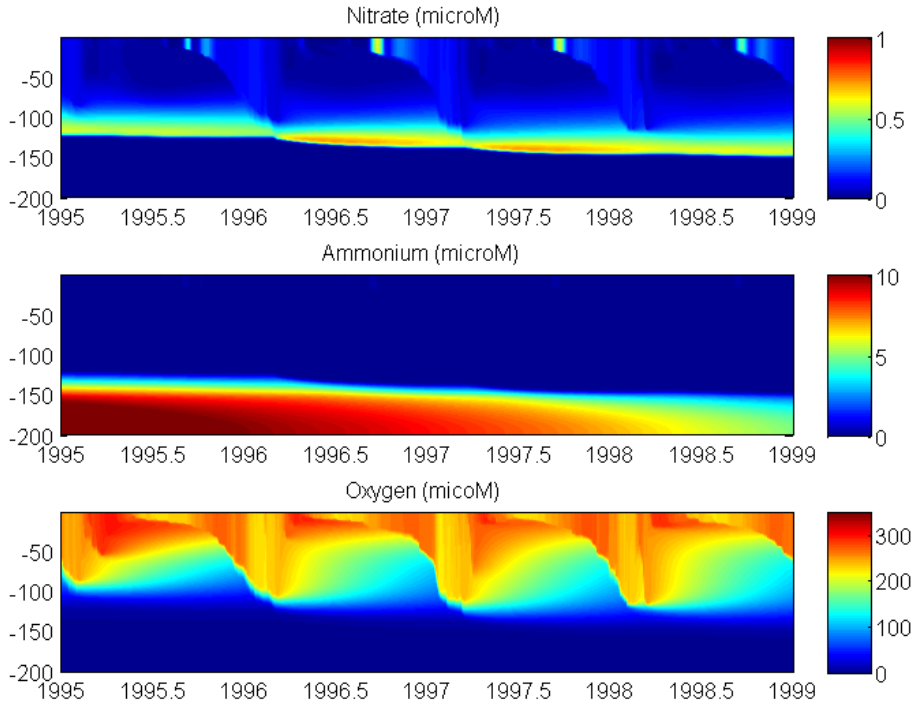


***Figure 7a.*** *Time evolution of chemical (nutrients and oxygen) variables during five years of the 1D simulation*

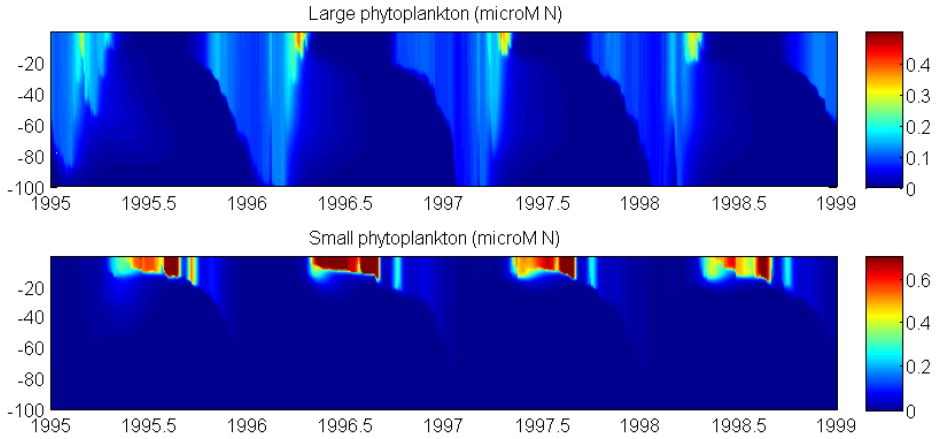


***Figure 7b.*** *Time evolution of phytoplankton (small and large) during five years of the 1D simulation*

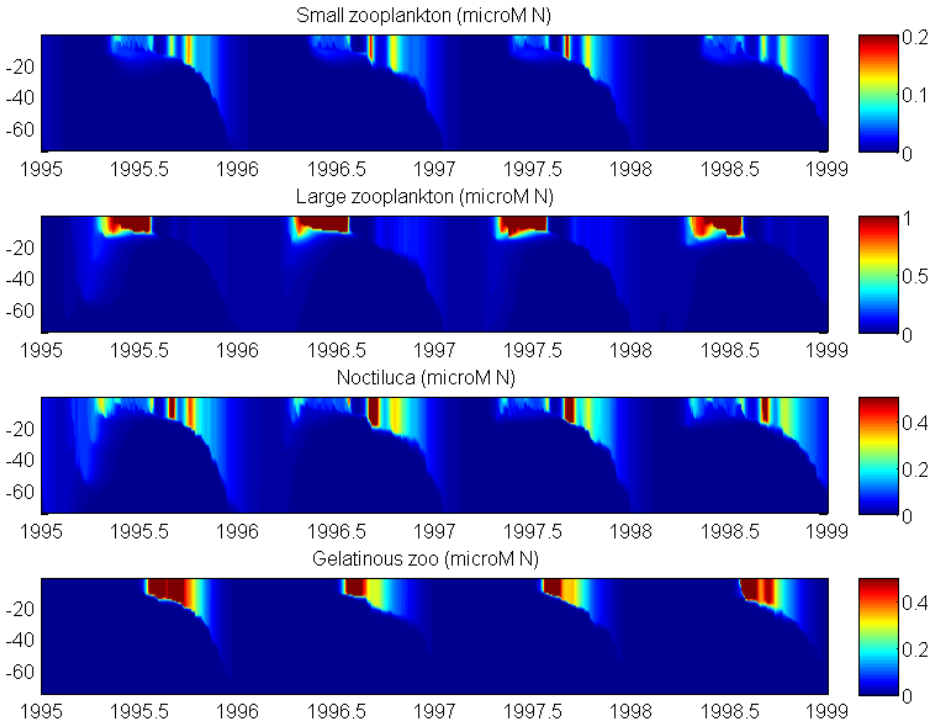


***Figure 7c**. Time evolution of zooplankton (all four types) during five years of the 1D simulation*

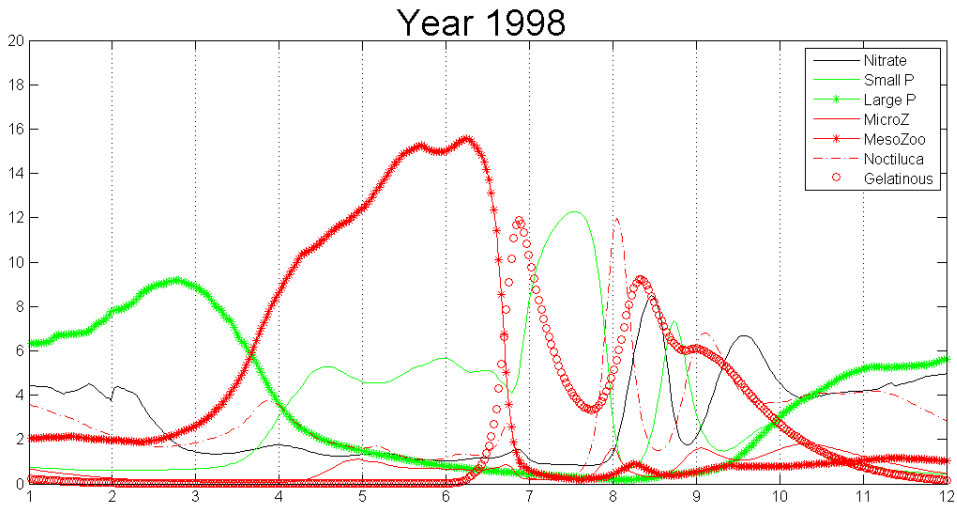


***Figure 7d**. Integrated values of biogeochemical variables in the upper 120 meters for year 1998*

## 3. **Conclusions**

During the 20 days visit of Prof. Oguz the basis for constructing the coupled physical ecosystem modelling system for the Black Sea has been established. At present the GETM/GOTM circulation model has been fine-tuned to provide realistic features of the

Black Sea circulation and thermohaline structure. The ecosystem model is implemented into the FABM coupling configuration to be linked to the GETM/GOTM circulation model. The one dimensional version of the ecosystem model excluding horizontal variations has already been implemented to the JRC model environment. The forthcoming efforts will be devoted to refining the coding system to include horizontal variability and to carry out further tests.

## Appendix A. BSSM model equations

The general form of equations governing the biogeochemical model is expressed by

$$\frac{\partial(X \cdot H)}{\partial t} + \nabla\left[\vec{u} \cdot (X \cdot H)\right] = F_X + R_X$$

where $X$ denotes each of the state variables, $\boldsymbol{u}$ is the three dimensional fluid velocity, $H = h + \eta$ the total water depth with h defining the bottom topography and η the surface elevation, $F_X$ denotes the sum of horizontal and vertical diffusion terms, and $R_X$ refers to the source-sink terms as described in a general form

$R_X$ = *Growth – Grazing – Excretion – (Respiration+Mortality)*

Except $R_X$, the mathematical forms of all terms in the equation above and their numerical solution procedures are similar to those of the temperature and salinity transport equations of the POM (Mellor, 2003). Detailed representation of source-sink terms is described below for each model compartment.

### A.1. The autotrophs

Temporal variations of the large ($P_L$) and small ($P_S$) phytoplankton biomass are governed by the biological source-sink terms of the form

$$R_{PX} = \sigma_X \cdot \Psi_X \cdot P_X - \sum G(P_X) \cdot Z_X - m_{PX} \cdot P_X \qquad \text{(A1a)}$$

where

$$\Psi_X = f_X(N_n, N_a) \cdot f_X(I) \cdot f_X(T) \qquad \text{(A1b)}$$

represents the total limitation function of the primary production, and the subscript $X$ denotes either $L$ for the large phytoplankton or $S$ for the small phytoplankton size group. The right hand side of eq. A1a describes, respectively, the phytoplankton growth (primary production), grazing by different zooplankton groups, and physiological mortality that also includes the respiration. This simplification is justified in the absence of explicit representation of the microbial loop. The phytoplankton growth is modeled as the products of phytoplankton bimass $P$ and the maximum specific growth rate $\sigma$. The growth, however, is subject to simultaneous limitations by the availability of nitrogen resource $f(N_n,N_a)$, the photosythetically available radiation $f(I)$, and temperature $f(T)$. Using a spectrally unresolved model, the light limitation is parameterized by (Jassby and Platt, 1976)

$$f_X(I) = \tanh\left[\alpha_X \cdot I\right] \cdot e^{-\beta_X I} \qquad \text{(A2a)}$$

$$I = I_S \cdot \exp\left\{-\mathrm{k_w z} - \int_0^z k_b(\mathrm{P_L} + \mathrm{P_S} + \mathrm{D}) \cdot dz\right\} \qquad \text{(A2b)}$$

where $\alpha_X$ is a parameter controlling slope of the photosynthesis-irradiance curve at low values of the photosynthetically available irradiance (PAR) whose surface intensity $I_S$ amounts to half of the incoming solar radiation, $\beta_X$ is the photoinhibition parameter to reduce the growth at high irradiance conditions. The light attenuation below the sea surface is represented by an exponential decay function in which the total light extinction coefficient $k$ comprises the contributions from sea water itself ($k_w$), and self-shading effects of phytoplankton and detritus material ($k_b$); $k = k_w + (P_L + P_S + D)k_b$.

The nitrogen limitation function comprises the sum of individual contributions of the ammonium and nitrate limitations; $f_X(N_n,N_a) = f_X(N_n) + f_X(N_a)$. They are expressed by the Monod-type hyperbolic functions involving a saturation response at high resource concentrations

$$f_X(N_a) = \left[\frac{N_a}{K_{AX} + N_a}\right] \quad \text{and} \quad f_X(N_n) = \left[\frac{N_n}{K_{NX} + N_n}\right] \cdot \left[\frac{K_{AX}}{K_{AX} + N_a}\right] \qquad \text{(A3a,b)}$$

where $N_a$ and $N_n$ denote ammonium and nitrate concentrations, respectively; $K_{AX}$ and $K_{NX}$ are the corresponding half saturation constants of ammonium and nitrate uptakes. The term within the second square brackets of eq. A3b represents the ammonium limitation of the nitrate uptake due to preferred consumption of ammonium in the growth process. The silicate control on the diatom growth is neglected as the available data does not yield evidence for the prevailing role of silicate limitation although its input from major rivers tends to decline during the last two decades. The temperature control of the form

$$f_L(T) = Q_{10}^{(12-T)/12} \qquad \text{(A3c)}$$

is imposed for the growth of large phytoplankton group to promote its growth at low temperatures but to reduce at high temperatures. No temperature control is imposed for the small phytoplankton group, but lower growth rate of the large phytoplankton group at high temperatures gives indirectly the small phytoplankton group a growth advantage.

### A.2. The heterotrophs and carnivores

Changes in the zooplankton biomass are controlled by ingestion, predation, excretion, and mortality which are expressed by

$$R(Z_S) = \gamma_Z G_S(P_S) Z_S - \left[G_L(Z_S) Z_L + G_N(Z_S) Z_N + G_G(Z_S) Z_G\right] - \mu_S Z_S - m_S Z_s^2 \qquad \text{(A4a)}$$

$$R(Z_N) = \gamma_Z \left[G_N(P_L) + G_N(Z_S) + G_N(D_n)\right] Z_N - G_L(Z_N) Z_L - G_G(Z_N) Z_G - \mu_N Z_N - m_N Z_N^2 \qquad \text{(A4b)}$$

$$R(Z_L) = \gamma_Z \left[G_L(P_L) + G_L(Z_S) + G_L(Z_N) + G_L(D_n)\right] Z_L - G_G(Z_L) Z_G - \mu_L Z_L - m_L Z_L^2 \qquad \text{(A4c)}$$

$$R(Z_G) = \gamma_Z \left[G_G(Z_S) + G_G(Z_L) + G_G(Z_N)\right] Z_G - \mu_G Z_G - m_G \cdot Q_{10}^{(15-T)/5} \cdot Z_G^2 \qquad \text{(A4d)}$$

where the subscript $X$ denoting either $L$ for the large zooplankton or $S$ for the small zooplankton size group or $G$ for the gelatinous zooplankton group and $N$ for the *Noctiluca scintillans,* and $\gamma_Z$, $\mu_X$ and $m_X$ are, respectively, the coefficient of assimilation efficiency, the excretion rate and the natural mortality rate expressed in the quadratic form.

The ingestion terms within the square brackets are represented by the Michaelis-Menten (the so-called Holling type II) functional form in terms of the maximum rate $g_j$, the temperature limitation function $f_j(T)$, and the food capture efficiency coefficient $b_{j,i}$ for the food item $X_i$ by

$$G_j(X_i) = g_j f_j(T) \frac{b_{j,i} \cdot X_i}{K_j + \left[\sum_i b_{j,i} \cdot X_i\right]} \qquad \text{(A5a)}$$

where the terms within the square bracket in the denominator refer to the total food available for the consumption of any zooplankton group, and $K_j$ denotes its half saturation value. The food preference coefficients are expressed as a function of the relative proportion of the total food by

$$b_{j,i} = \frac{a_{j,i} \cdot P_i}{\sum_i a_{j,i} \cdot P_i} \qquad \text{(A5b)}$$

where $a_{j,i}$ denotes the constant food preference coefficient specified externally as in Table A4. According to eq. A5a,b, when a food type declines, its grazing preference decreases (Gentleman et al., 2003) . In this case, zooplankton select an alternative food type having higher biomass. Thus, grazing preferences may switch from one prey to another depending on local conditions and the predator may select temporally and spatially most favorable food types.

The temperature control of the growth, $f_j(T)$, is introduced for the *Noctiluca* and the gelatinous groups in the form

$$f_{ZN}(T) = Q_{10}^{(T-12)/8} \qquad \text{(A6a)}$$

$$f_{ZG}(T) = Q_{10}^{(T-20)/4} \quad for \quad T > 20 \quad and \quad f_{ZG}(T) = 1 \quad otherwise \qquad \text{(A6b)}$$

According to the observations, Noctiluca can maintain its growth at a wide temperature range of 12-30$^o$C. Eq. A6a supresses the *Noctiluca* growth at low temperatures but favors it in spring and summer months when the surface mixed layer starts warming up. Eq. A6b imposes the growth advantage of *Mnemiopsis leidyi* population at high temperatures during July-August, whereas the lower growth rate values at lower temperatures support the jellyfish *Aurelia aurita* population growth.

### A.3. Particulate organic nitrogen (PON)

Egestion and sloppy feeding (i.e. unassimilated part of the food grazed) given by eq. A7a and phytoplankton and zooplankton mortalities in eq. A7b form the detritus sources. Its consumption by zooplankton groups within the water column (eq. A7c) and transformation into the dissolved organic nitrogen pool at a rate $\varepsilon_n$ constitutes the sinks of detritus.

$$\begin{aligned} DETR1 = {} & (1-\gamma_Z)G_S(P_S)Z_S + (1-\gamma_Z)[G_N(P_L) + G_N(Z_S)]Z_N \\ & + (1-\gamma_Z)[G_L(P_L) + G_L(Z_S) + G_L(Z_N)]Z_L \\ & + (1-\gamma_Z)[G_G(Z_S) + G_G(Z_L) + G_G(Z_N)]Z_G \end{aligned} \qquad \text{(A7a)}$$

$$DETR2 = \left[ \sum_k m_{Pk} P_k + \sum_k m_k Z_k^2 \right] \qquad \text{(A7b)}$$

$$DETR3 = \gamma_Z \cdot [G_L(D_n)Z_L + G_N(D_n)Z_N] \qquad \text{(A7c)}$$

The total source-sink terms for the detritus equation is given by

$$R(D_n) = DETR1 + DETR2 - DETR3 - \varepsilon_n D_n \qquad \text{(A7d)}$$

Following the chemical reactions in Eq. 12a-c, the decomposition rate of particulate organic nitrogen is represented by

$$\varepsilon_n(DO) = \varepsilon_{n0}\left[1 + \frac{R_0}{R_0 + DO}\right] \quad for \quad DO < 250\mu M$$
$$\varepsilon_n(DO) = \varepsilon_{n0} \quad otherwise \qquad \text{(A7e)}$$

which implies twice higher decomposition rate in the oxygen deficient part of the water column due to more active bacterial processes with respect to the surface aerobic layer.

### A.4. Dissolved inorganic nitrogen (DIN)

The changes in ammonium and nitrate concentrations are expressed by

$$R(N_a) = \varepsilon_n D_n + \sum_k \mu_{zk} \cdot Z_k - \left[ \sum_k \sigma_k \cdot f_k(T) \cdot f_k(I) \cdot f_k(N_a) \cdot P_k \right] - r_n \cdot N_a - r_a \cdot N_a \cdot N_n - r_b \cdot N_a \quad \text{(A9a)}$$

$$R(N_n) = r_n \cdot N_a - \left[ \sum_k \sigma_k \cdot f_k(T) \cdot f_k(I) \cdot f_k(N_n) \cdot P_k \right] - 0.8 \cdot \varepsilon_n \cdot D_n - \frac{3}{5} r_a \cdot N_a \cdot N_n - \frac{4}{3} r_s \cdot HS \cdot N_n \quad \text{(A9b)}$$

In eq. A9a, the first and second terms represent ammonium sources due to decomposition of PON and zooplankton excretion, respectively. The third term represents its uptake during the primary production and the last two terms are the ammonium oxidation by oxygen and nitrate following the reactions in Eqs. A13a,b. According to eq. A9b, the only internal source of nitrate is its recycled form due to the oxidation of ammonium (the first term). Nitrate concentration is consumed due to its uptake (the second term), anaerobic particulate matter remineralization following eq. 12b (the third term) that applies at oxygen concentrations less than *100 μM*, the oxidations of ammonium and hydrogen sulphide taking place at oxygen concentrations less than *20 μM* following eq's A13b,d.

### A.5. Dissloved oxygen and hydrogen sulphide

Dissolved oxygen concentration is altered by a balance between its photosynthetic production by the autotrophs and the consumption due to the pelagic decomposition of organic matter (eq. A12a), the excretion of zooplankton as well as the oxidation of ammonium (eq. A13a) within the oxygenated parts of the water column ($O_2$ > 10 μM) and oxidation of hydrogen sulphide near the anoxic interface (eq. A13d), as given by

$$R(DO) = 8.125 \left[ \sum_k \Psi_k \cdot P_k \right] - 6.625 \left[ \varepsilon_n \cdot D_n + \sum_k \mu_{zk} \cdot Z_k \right] - 2 r_n \cdot N_a - \frac{1}{2} r_o \cdot HS \cdot DO \quad \text{(A11a)}$$

The air-sea exchanges of surface dissolved oxygen concentration is given by

$$K_v \frac{\partial DO}{\partial z} = -V_p \cdot \left[ DO_{sat} - DO(z=0) \right] \quad \text{(A11b)}$$

where $K_v$ is the vertical diffusivity, $DO_{sat}$ represents the oxygen saturation concentration computed according to the UNESCO formula (1996) , and $V_p$ is the gas transfer velocity computed according to the relation given by Wanninkhof (1992).

The reaction kinetics governing temporal changes of hydrogen sulphide concentration are given by

$$R(HS) = 0.5 \cdot \varepsilon_n \cdot D_n - r_o \cdot HS \cdot DO - r_s \cdot HS \cdot N_n - r_u \cdot HS \quad \text{(A11c)}$$

where the first term signifies hydrogen sulphide production by the process of sulfate based anaerobic organic matter decomposition (Eqs. A12c), the second and third terms express the oxidation reactions of $H_2S$ by oxygen and nitrate (Eqs. A13c,d), respectively.

### A.6. Restoring terms

A peculiar observed feature of the Black Sea biogeochemical structure is the coincidence of the subsurface nitrate peak permanently to 15.5 ± 0.2 kg $m^{-3}$ isopycnals although its location may vary in terms of depth. The mechanism controlling this process is unclear and therefore this feature can not be simulated with precision in the model. In order to maintain this feature in the model, a restoring term is used to restore the model computed nitrate concentrations to their observed values at the narrow density range of 15.2 - 15.7 kg $m^{-3}$. Similarly, we restore ammonium and hydrogen sulphide concentrations of the model to their observations within the anoxic layer, because the redox processes governing the deep anoxic pool are not modeled expicitly as they are not main concern of this study. The restoring is also used for maintaining less saline coastal water mass around the basin at depths shallower than 200m. The general form of the restoring terms is given by

$$\frac{\partial X}{\partial t} = \left[other \quad terms\right] + \frac{1}{\tau_X}(X_{obs} - X) \qquad \text{(A11)}$$

where $X$ is a model parameter, $X_{obs}$ its observed value, $\tau_X$ is the restoring time scale set to 20 days.

### A.7. Redox reactions

The organic matter is decomposed in different parts of the water column following the reactions

$$OM + 130O_2 = xCO_2 + yNH_3 + H_3PO_4 + xH_2O$$

$$OM + 0.8 * xHNO_3 = xCO_2 + yNH_3 + H_3PO_4 + 1.4 * xH_2O + 0.4 * xN_2 \qquad \text{(A12a-d)}$$

$$OM + 0.5 * xSO_4^{2-} = xCO_2 + yNH_3 + H_3PO_4 + 0.5 * xH_2S$$

*where*

$$OM = \left(CH_2O\right)_x \left(NH_3\right)_y H_3PO_4$$

and x=106 and y=16 denote the Redfield stoichiometic coefficients for the molar C:P and N:P ratios, respectively. For more extensive description of the stoichiometries of remineralisation and denitification processes, we refer to Neumann (2000), Soataert et al. (2007), and Paulmier et al. (2009).

Ammonium is oxidized by oxygen within the aerobic part of the water column to form the dissolved inorganic nitrate (i.e. the nitrification process). It is also oxidized by nitrate within the suboxic zone to prevent its upward flux from the anoxic pool into the euphotic zone. The reactions for these processes are given by

$$NH_4 + 2O_2 = NO_3 + 2H^+ + H_2O \qquad \text{(A13a)}$$

$$NH_4 + 3/5NO_3 = 4/5N_2 + 9/5H_2O + 2/5H^+ \qquad \text{(A13b)}$$

Hydrogen sulphide is oxidized near the anoxic interface by oxygen and nitrate following the reactions

$$H_2S + \frac{1}{2}O_2 = S^0 + H_2O \quad \text{(A13c)}$$

$$H_2S + 4/3NO_3 + 2OH^- = SO_4^{\ 2} + 2/3N_2 + 2H_2O \quad \text{(A13d)}$$

Table A1. Definition of parameters and their values used for the phytoplankton groups

| Definition | Unit | Large Phyto | Small Phyto |
|---|---|---|---|
| Maximum growth/ grazing rate | $d^{-1}$ | $\sigma_L$=1.2 | $\sigma_S$=1.0 |
| Half saturation constant for nitrate uptake | mmol N $m^{-3}$ | $K_{NL}$=0.5 | $K_{NS}$=0.3 |
| Half saturation constant for ammonium uptake | mmol N $m^{-3}$ | $K_{AL}$=0.3 | $K_{AS}$=0.2 |
| Mortality rate | $d^{-1}$ | $m_{PL}$=0.05 | $m_{PS}$=0.06 |

Table A2. Definition of parameters and their values used for the zooplankton groups

| Definition | Unit | Microzoo | Mesozoo | Noctiluca | Gelatinous |
|---|---|---|---|---|---|
| Maximum grazing rate | $d^{-1}$ | $g_{ZS}$ =0.8 | $g_{ZL}$ =0.5 | $g_{ZN}$ =0.5-1 | $g_{ZG}$=0.15-0.6 |
| Half saturation constant | mmol $m^{-3}$ | $K_{ZS}$=0.4 | $K_{ZL}$=0.5 | $K_{ZN}$=0.4 | $K_{ZG}$=0.25 |
| Mortality rate | (mmol $m^{-3}$)$^{-1}$ $d^{-1}$ | $m_{ZS}$=0.1 | $m_{ZL}$=0.15 | $m_{ZN}$=0.1 | $m_{ZG}$=0.15 |
| Excretion rate | $d^{-1}$ | $\mu_{ZS}$=0.04 | $\mu_{ZL}$=0.05 | $\mu_{ZN}$=0.06 | $\mu_{ZG}$=0.06 |

Table A3. Definition of additional parameters and their values

| Definition | Unit | Value |
|---|---|---|
| Light extinction coefficient for PAR in pure water | $m^{-1}$ | $k_w$=0.07 |
| Self-shading coefficient of the light extinction | $m^{-1}$ mmol $m^{-3}$ | $k_b$=0.01 |
| Light attenuation coefficient for the large phyto | $m^2$ $W^{-1}$ | $\beta_{PL}$=0.0015 |
| $Q_{10}$ factor of the temperature control | unitless | $Q_{10}$=2 |
| Assimilation efficiency of food grazing | unitless | $\gamma_Z$=0.7 |
| Maximum detritus sinking rate | m $d^{-1}$ | $W_D$=10.0 |
| Remineralization rate for particulate nitrogen | $d^{-1}$ | $\varepsilon_n$=0.05 |
| Nitrification rate | $d^{-1}$ | $r_{n,max}$ =0.2 |
| Ammonium oxidation rate by nitrate in the SOL | $d^{-1}$ | $r_a$ =0.1 |
| Ammonium oxidation rate by other processes in the SOL | $d^{-1}$ | $r_b$ =0.1 |
| Hydrogen sulphide oxidation rate by nitrate in the SOL | $d^{-1}$ | $r_s$ =0.1 |
| Hydrogen sulphide oxidation rate by oxygen in the SOL | $d^{-1}$ | $r_o$ =0.1 |
| Hydrogen sulphide oxidation rate by other processes | $d^{-1}$ | $r_u$ =0.1 |

Table A4. Food capture efficiency parameters of the zooplankton groups

| | Microzoo | Mesozoo | Noctiluca | Gelatinous |
|---|---|---|---|---|
| Large phytoplankton | -- | 1.0 | 0.5 | -- |
| Small phytoplankton | 1.0 | -- | 0.5 | -- |
| Detritus | -- | 0.5 | 1.0 | -- |
| Microzooplankton | -- | 0.5 | 0.25 | 1.0 |
| Mesozooplankton | -- | -- | -- | 0.5 |
| Noctiluca | -- | 0.25 | -- | 0.3 |

European Commission
EUR 27003 EN – Joint Research Centre – Institute for Environment and Sustainability

Title: Development of the Black Sea specific ecosystem model (BSSM)

Author(s): Temel Oguz, Adolf Stips, Diego Macias, Elisa Garcia-Gorriz, Clare Coughlan

Luxembourg: Publications Office of the European Union

2014 – 25 pp. – 21.0 x 29.7 cm

EUR – Scientific and Technical Research series – ISSN 1831-9424 (online)

ISBN 978-92-79-44670-2 (PDF)

doi:10.2788/82470

LB-NA-27003-EN-N

## JRC Mission

As the Commission's in-house science service, the Joint Research Centre's mission is to provide EU policies with independent, evidence-based scientific and technical support throughout the whole policy cycle.

Working in close cooperation with policy Directorates-General, the JRC addresses key societal challenges while stimulating innovation through developing new methods, tools and standards, and sharing its know-how with the Member States, the scientific community and international partners.

*Serving society*
*Stimulating innovation*
*Supporting legislation*

doi:10.2788/82470

ISBN 978-97-79-44670-2

Publications Office